

Parameters of Defect Mode of 1D Microwave Waveguide Photonic Crystal with Metal Inclusions in the Element That Disturbs Periodicity

D. A. Usanov*, A. V. Skripal', and A. A. Romanov

Chernyshevsky State University, Saratov, 410012 Russia

**e-mail: usanovda@info.sgu.ru*

Received May 18, 2016

Abstract—Amplitude–frequency characteristics of the transmission coefficient of microwave waveguide photonic crystal with violation of periodicity are studied in the presence of a plane conducting small-size inclusion that occupies a part of the transverse cross section of the waveguide inside a disturbed layer located at different positions. The conducting small-size inclusion in the disturbed layer of photonic crystal causes the low-frequency shift of the defect mode in the band gap, and the maximum shift is observed when the metal inclusion is located at the interface or center of disturbance depending on the thickness of the disturbed layer.

DOI: 10.1134/S1063784217060263

INTRODUCTION

Recent progress in the development of microwave devices is related to the application of periodic structures known as photonic crystals [1–3]. Such structures are periodic structures consisting of elements the sizes of which are comparable with the wavelength of the propagating electromagnetic radiation. The spectrum of such a structure exhibits a frequency band in which the propagation of electromagnetic waves is impossible (analog of the band gap in crystals). Disturbances of the periodicity of the layered structure lead to the formation of narrow resonant transparency windows in the band gap of the photonic crystals (defect modes) [4, 5].

Practical applications of microwave photonic crystals in highly directional resonant antennas, resonant cavities for semiconductor detectors, and various microwave filters (including filters with controlled parameters) have been analyzed in [1, 6–10].

The methods for the measurement of parameters of semiconductor structures using microwave photonic crystals are based on the assumption that the structure under study completely fills the transverse cross section of the waveguide [11–13]. In this case, the structure under study provides a significant variation in the amplitude–frequency characteristics (AFCs) of the photonic crystals and, hence, relatively high resolution and sensitivity with respect to the measured parameters can be reached. However, the measurement locality is limited by the area of the transverse cross section of the waveguide and better locality can

be obtained using waveguides with higher frequencies, which may lead to technical problems.

When the structure under study occupies a part of the transverse cross section of the photonic crystal waveguide, the enhancement of the response of the photonic-crystal AFC to the measured parameters necessitates the analysis of the effect of the structure parameters and position in the preliminary fabricated inhomogeneity that serves as a microcavity in the photonic crystal [14]. The results of [15] show that multiple air cavities in the disturbed layer lead to variations in the AFCs of the transmittance of the photonic crystal (in particular, high-frequency shift of the transmission peak in the band gap, i.e., variation in the frequency of the defect mode). In this case, the AFC of the photonic crystal can be analyzed using the model of effective medium. Metal impurities (and the corresponding variations in the parameters of the defect mode) may serve as an alternative to air cavities in the control of the AFC of photonic crystal.

The purpose of this work is the study of variations in the AFC of the transmittance of microwave photonic crystal with disturbed periodicity in the presence of conducting small-size plane inclusion that occupies a part of the transverse cross section of the waveguide in the disturbed layer.

MODEL OF WAVEGUIDE PHOTONIC CRYSTAL

We study the waveguide photonic crystal that consists of 11 layers in a frequency interval of 8–12 GHz

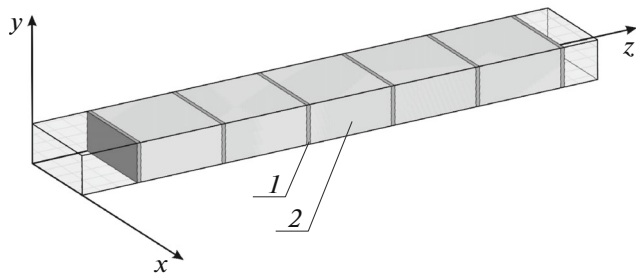


Fig. 1. 3D model of a periodic waveguide photonic crystal: (1) ceramic (Al_2O_3) layer and (2) Teflon.

(Fig. 1). Odd layers are made of ceramic material (Al_2O_3 with $\epsilon = 9.6$), and even layers are made of Teflon ($\epsilon = 2.0$). The layer thicknesses are $d_{\text{Al}_2\text{O}_3} = 1$ mm and $d_{\text{tef}} = 22$ mm. The layers completely fill the transverse cross section of the waveguide.

The layer sizes are chosen in such a way that the band gap of the photonic crystal is located at the center of the frequency interval under study (8–12 GHz).

The periodicity of the photonic structure is violated due to the presence of the central (sixth) layer with thickness $d_{\text{tef}} = 2.3$ or 14.5 mm.

A metal inclusion (a square aluminum plate with a thickness of 100 μm and side $a_{\text{met}} = 3$ mm) is placed inside the disturbed layer at the center of the waveguide cross section (Fig. 2).

COMPUTER SIMULATION

Numerical simulation using software for the 3D simulation of electromagnetic fields with the aid of the ANSYS HFSS finite-element method is employed for the study of the AFC of the transmittance of photonic crystal with violated periodicity in the presence of metal inclusion inside the disturbed layer.

As was mentioned, disturbances of the periodicity of the photonic crystal lead to the formation of the defect mode on the AFC of the transmission coefficient.

To study the effect of the position of the metal inclusion (aluminum film) in the disturbed layer that serves as the microcavity in the photonic crystal on the parameters of the defect mode [6, 10] or transparency window [7], we calculate distributions of the electric field of electromagnetic wave at the frequency of the defect mode.

Figure 3 presents the calculated distributions of the field at the frequency of the defect mode.

The calculations of the electric field of electromagnetic wave show alternation of wave nodes and antinodes inside the photonic crystal along the propagation direction. For the above parameters of the photonic crystal in the absence of the metal inclusion, a

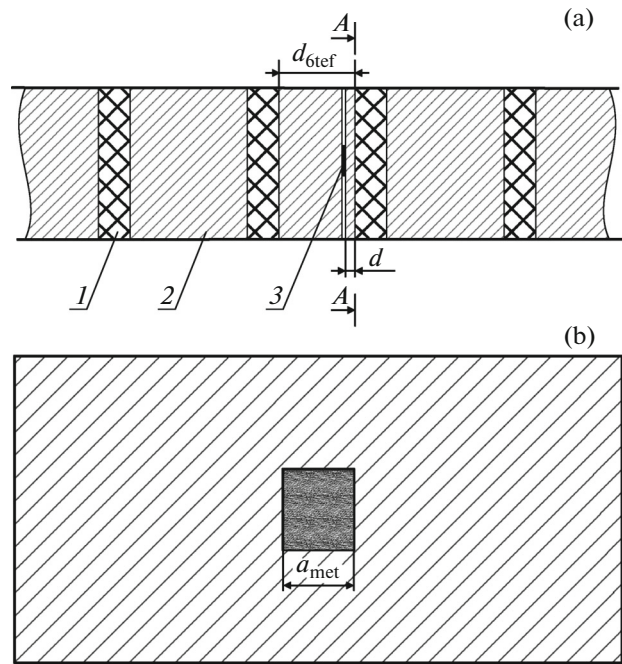


Fig. 2. Position of metal inclusion (aluminum film) inside the disturbed layer in the waveguide on (a) longitudinal and (b) transverse cross sections of the waveguide: (1) Al_2O_3 layer with a thickness of 1 mm, (2) Teflon layer with a thickness of 22 mm, and (3) metal inclusion in the disturbed layer located at distance d from the Al_2O_3 layer.

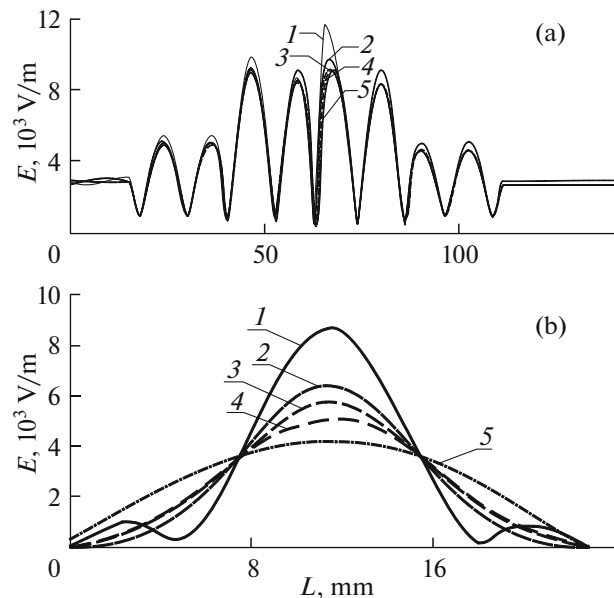


Fig. 3. Distribution of electric field of electromagnetic wave inside photonic crystal (a) along the propagation direction and (b) in the transverse plane ($A-A$ plane in Fig. 2) for several positions of metal inclusion in the inhomogeneity ($d = (1) 0$, (2) 100, (3) 200, and (4) 300 μm) and (5) in the absence of the metal inclusion at $f_{\text{res}} = 10.095$ GHz and $d_{6\text{tef}} = 2.3$ mm.

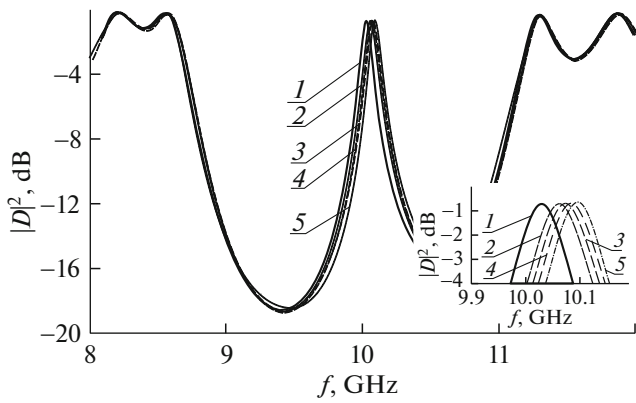


Fig. 4. AFCs of the photonic crystal at several positions of the metal inclusion with a size of $a_{\text{met}} = 3$ mm inside the inhomogeneity ($d = (1) 0$, (2) 100, (3) 200, and (4) 300 μm) and (5) in the absence of the metal inclusion.

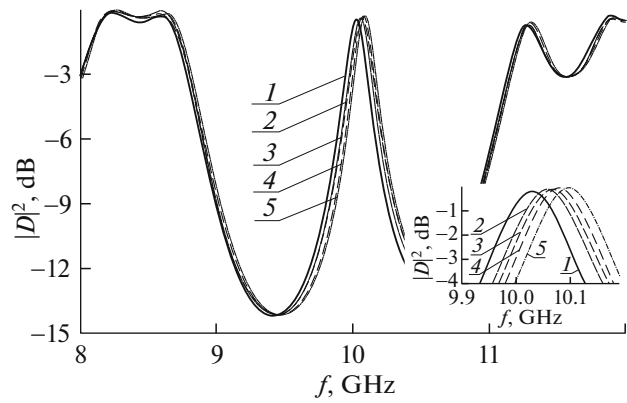


Fig. 5. Experimental AFCs of the photonic crystal at several positions of the metal inclusion with a size of $a_{\text{met}} = 3$ mm inside the inhomogeneity ($d = (1) 0$, (2) 100, (3) 200, and (4) 300 μm) and (5) in the absence of the metal inclusion.

node is observed at defect-mode frequency f_{res} at the center of the disturbed layer (curve 5 in Fig. 3).

Figure 3 shows that the presence of the metal inclusion (aluminum film) in the disturbed layer of the photonic crystal leads to the distortions of the electric field distribution and the maximum distortion is observed when the metal inclusion is located at the interface of the disturbed layer.

Such a variation in the distribution of the electric field may cause variations in the position of the resonant feature in the band gap of the photonic crystal.

Figure 4 presents the calculated results for the AFC of the photonic crystal at several positions of the metal inclusion with a size of $a_{\text{met}} = 3$ mm inside the inhomogeneity. The inset to Fig. 4 shows the AFCs of the photonic crystal in the vicinity of the defect-mode frequency in the band gap of the photonic crystal.

The analysis of the curves shows that the presence of the metal inclusion in the inhomogeneity leads to the low-frequency shift of defect-mode frequency f_{res} of the photonic crystal relative to defect-mode frequency f_0 in the absence of the metal inclusion. Note that the maximum shift $\Delta f = f_{\text{res}} - f_0 = 63$ MHz is reached when the inclusion is located at the interface of the disturbed layer ($d = 0$) and the shift decreases when the metal inclusion is shifted to the center of inhomogeneity ($\Delta f = 13$ MHz at $d = 300$ μm). The minimum shift is reached when the metal inclusion is located at the center of the inhomogeneity ($d = 1.15$ mm).

The calculations show that the defect mode generated at a thickness of $d_{\text{def}} = 2.3$ mm ($d_{\text{def}} < \lambda_{\text{res}}/2$, where λ_{res} is the wavelength at the defect-mode frequency) can also be obtained at a greater thickness of $d_{\text{def}} = 14.5$ mm ($\lambda_{\text{res}}/2 < d_{\text{def}} < \lambda_{\text{res}}$). At the greater thickness, we observe significant redistribution of electric field of electromagnetic wave inside the pho-

tonic crystal along the direction of propagation at the defect-mode frequency that leads to the antinode of the electric field at the center of the disturbed layer.

The analysis of the AFC of the photonic crystal with a thickness of $d_{\text{def}} = 14.5$ mm shows that the presence of metal inclusion in the inhomogeneity also leads to the low-frequency shift of the defect-mode frequency of the photonic crystal. The maximum (minimum) shift is reached when the inclusion is located at the center of the disturbed layer (interface of inhomogeneity).

EXPERIMENT

We experimentally study the photonic crystal that is fabricated in accordance with the above model and represents alternating ceramic and Teflon layers. The AFC of the transmittance of the photonic crystal is measured in the 3-cm-wavelength range using an Agilent PNA-L Network Analyzer N5230A.

Figure 5 shows the experimental AFCs of the photonic crystal for several positions of the metal inclusion with a fixed size of $a_{\text{met}} = 3$ mm inside the inhomogeneity with a size of 2.3 mm. The inset to Fig. 5 presents the AFCs of the photonic crystal in the vicinity of the defect-mode frequency of the photonic crystal.

The comparison of the calculated and experimental AFCs (Figs. 4 and 5) of the photonic crystal at several positions of the metal inclusion inside the inhomogeneity at $d_{\text{def}} = 2.3$ mm yields quantitative agreement and proves the minimum and maximum shifts for the inclusions located at the center of the disturbed layer and the interface of inhomogeneity, respectively.

The measurements of the AFCs of the photonic crystal with the greater (14.5 mm) thickness of the central disturbed layer prove the simulated results and show that the minimum and maximum shifts of the

defect mode are reached for the metal inclusions located at the interface of inhomogeneity and the center of the disturbed layer, respectively.

CONCLUSIONS

Effect of a plane metal small-size inclusion in the layer that destroys periodicity of a microwave photonic crystal on the AFC of the transmission coefficient is numerically simulated and experimentally studied.

The presence of the plane conducting small-size inclusion in the disturbed layer of the photonic crystal causes the low-frequency shift of the defect mode in the band gap. The maximum shift is obtained when the metal inclusion is located at the interface of inhomogeneity at the disturbed layer thickness $d_{\text{def}} < \lambda_{\text{res}}/2$ and at the center of inhomogeneity at $\lambda_{\text{res}}/2 < d_{\text{def}} < \lambda_{\text{res}}$. The results can be used for the development of microwave photonic crystals with electrically controlled parameters.

ACKNOWLEDGMENTS

This work was supported by the Ministry of Education and Science of the Russian Federation (project nos. 1376 and 1575).

REFERENCES

1. E. Ozbay, B. Temelkuran, and M. Bayindir, *Prog. Electromagn. Res.* **41**, 185 (2003).
2. A. Gomez, A. Vegas, M. A. Solano, and A. Lakhtakia, *Electromagnetics* **25**, 437 (2005).
3. Yu. V. Gulyaev and S. A. Nikitov, *Radiotekhnika*, No. 8, 26 (2003).
4. E. Yablonovitch, T. J. Gmitter, and R. D. Meade, *Phys. Rev. Lett.* **67**, 3380 (1991).
5. D. Usanov, A. Skripal, A. Abramov, A. Bogolubov, V. Skvortsov, and M. Merdanov, in *Proc. 37th European Microwave Conf., Munich, Germany, 2007*, p. 198.
6. G. W. Burns, I. G. Thayne, and J. M. Arnold, in *Proc. European Conf. on Wireless Technology, Amsterdam, Netherlands, 2004*, p. 229.
7. H.-S. Wu and C.-K. C. Tzuang, in *Proc. 34th European Microwave Conf., Amsterdam, Netherlands, 2004*, Vol. 2, p. 1189.
8. B. A. Belyaev, A. S. Voloshin, and V. F. Shabanov, *Dokl. Phys.* **50**, 337 (2005).
9. I. B. Vendik and O. G. Vendik, *Tech. Phys.* **58**, 1 (2013).
10. D. A. Usanov, M. K. Merdanov, A. V. Skripal', and D. V. Ponomarev, *Izv. Sarat. Gos. Univ. Nov. Ser. Ser. Fiz.* **15**, 57 (2015).
11. D. A. Usanov, A. V. Skripal', A. V. Abramov, A. S. Bogolyubov, V. S. Skvortsov, and M. K. Merdanov, *Izv. Vyssh. Uchebn. Zaved., Elektron.*, No. 6, 25 (2007).
12. Yu. V. Gulyaev, S. A. Nikitov, D. A. Usanov, A. V. Skripal', A. E. Postel'ga, and D. V. Ponomarev, *Dokl. Phys.* **57**, 145 (2012).
13. D. A. Usanov, A. V. Skripal, D. V. Ponomarev, E. V. Latsheva, and S. A. Nikitov, in *Proc. 44th European Microwave Conf., Rome, Italy, 2014*, p. 984.
14. I. D. Joannopoulos, P. R. Villeneuve, and S. Fan, *Nature* **386** (13), 143 (1997).
15. D. A. Usanov, A. V. Skripal', M. K. Merdanov, and V. O. Gorlitskii, *Tech. Phys.* **61**, 221 (2016).

Translated by A. Chikishev